



Measurement of the d_{36} coefficient of mercury cadmium telluride by reflection second harmonic generation

A. W. Wark, D. Pugh, L. E. A. Berlouis, F. R. Cruickshank, and P. F. Brevet

Citation: *Journal of Applied Physics* **89**, 306 (2001); doi: 10.1063/1.1330246

View online: <http://dx.doi.org/10.1063/1.1330246>

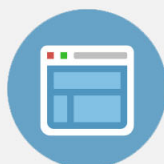
View Table of Contents: <http://scitation.aip.org/content/aip/journal/jap/89/1?ver=pdfcov>

Published by the [AIP Publishing](#)



Re-register for Table of Content Alerts

Create a profile.



Sign up today!



Measurement of the d_{36} coefficient of mercury cadmium telluride by reflection second harmonic generation

A. W. Wark, D. Pugh, L. E. A. Berlouis,^{a)} and F. R. Cruickshank

Department of Pure and Applied Chemistry, University of Strathclyde, Glasgow G1 1XL, United Kingdom

P. F. Brevet

Laboratoire d'Electrochimie, École Polytechnique Fédérale de Lausanne, CH-1015 Lausanne, Switzerland

(Received 18 April 2000; accepted for publication 2 October 2000)

The second order nonlinear coefficient (d_{36}) of the narrow band gap semiconductor, mercury cadmium telluride (MCT), is measured. Because MCT is strongly absorbing at a 1.06 μm wavelength, the measurement was performed by comparing the second harmonic intensity reflected from the material surface to the second harmonic intensity measured for a quartz sample in transmission. The analysis depends on the derivation of comparable expressions for the reflected and transmitted intensities. Using this approach a value of $d_{36} = 350 \pm 40$ pm/V is obtained, a value much larger than those reported for similar zinc-blende type materials. The large magnitude of the MCT d_{36} is attributed to an electronic resonance enhancement. © 2001 American Institute of Physics. [DOI: 10.1063/1.1330246]

INTRODUCTION

Knowledge of the absolute value of the second order nonlinear optical coefficient of materials plays a key role in assessing their performance. However, for materials which are strongly absorbing at both the fundamental and the second harmonic (SH) frequencies, nonlinear optical characterization using techniques such as the well-established Maker Fringe method,¹ in which the transmitted SH waves are measured, cannot be used. It is therefore necessary to establish alternative methods to allow an accurate measurement of nonlinear optical parameters such as the d coefficients through measurement of the reflected SH intensity. Previous studies by Hase *et al.*² on the reflected SH signal from a ZnSe layer deposited on GaAs demonstrated that the occurrence of multiple reflections within the thin ZnSe film significantly enhances the radiated SH signal. By normalizing this SH signal with respect to the signal from a GaAs substrate in reflection, an estimate of the d_{36} coefficient of ZnSe was made. Also, in work by Fluegel *et al.*,³ the reflected SH signal from an ordered $\text{Ga}_{1-x}\text{In}_x\text{P}$ surface was quantified with respect to the signal reflected from a GaAs surface. However, in neither of these cases (nor to our knowledge in any other) has a direct comparison been made between the measurement of the SH intensity for a sample in reflection and the intensity obtained for the same sample (or for a well-documented material such as quartz) in transmission. Such an approach would be useful for testing the theoretical understanding of the reflected and the transmitted responses.

Reflected second harmonic radiation at the input surface of a noncentrosymmetric material will in general be made up of contributions from specific surface effects and from an effect that depends only on the bulk second order susceptibility. The latter contribution necessarily occurs if the SH

wave boundary conditions are to be satisfied. It is relatively easy to make approximate calculations of the bulk contribution and in many cases⁴ this is predicted to be very small. This has been confirmed in experiments on crystals with known bulk d tensors, where, in comparison with transmitted intensities, the reflected SHG is found to be negligible or undetectable. Where a substantial amount of reflected SHG is detected, it will either be attributable to a specific surface effect or to an exceptionally large bulk coefficient. In semiconductor materials such as $\text{Hg}_{1-x}\text{Cd}_x\text{Te}$ (MCT), there is good reason to expect that very large effective d coefficients will be found because the experiments involve photon energies that are well above the optical band gap, so that considerable resonant enhancement is likely to be involved. In this article, we describe a scheme where the reflected SH wave was employed to measure accurately the d_{36} coefficient of the narrow band gap semiconductor, MCT.

EXPERIMENT

The MCT sample employed ($x=0.277$) was grown by the interdiffused multilayer process by metal organic vapor phase epitaxy (IMPMOVPE)⁵ on a vicinal GaAs (100) substrate, tilted towards the [110] direction (Fig. 1). MCT has a cubic zinc-blende structure with the second order susceptibility tensor having only one independent element, the d_{36} coefficient.⁶ To determine the magnitude of the effective d coefficient, it is necessary to compare the reflected SH intensity from the sample with that generated by a well-characterized reference material, in this case quartz. However, the SH intensity generated by the 1064 nm output of a Q-switched Nd:YAG laser (19 Hz repetition rate, 20 ns pulse width) at the quartz/air interface was too weak for comparison purposes. Thus it was necessary that the SH intensity was measured in transmission through the quartz and then compared with the intensity obtained in reflectance from the MCT material.

^{a)}Corresponding author. Phone: +44 141 548 4244; Fax: +44 141 548 4822; Electronic mail: L.Berlouis@strath.ac.uk

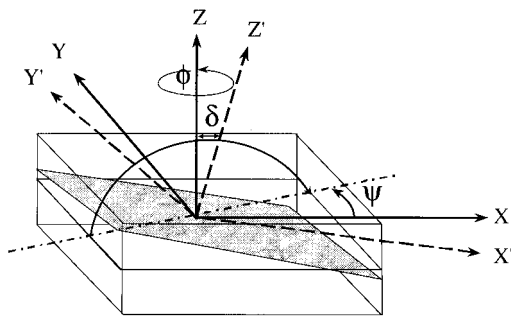


FIG. 1. Schematic representation of the vicinal MCT epitaxial layer grown on a GaAs (100) substrate, tilted towards the [110] direction.

In our experiments, the fundamental radiation was split into two beams. One beam was passed through a quartz reference, and the other either reflected off the MCT surface or transmitted through a second quartz slab. The intensity of the SH signal from both the reference and the sample was collected using two identical photomultiplier tubes (EMI 9813B), masked with 532 nm bandpass filters. The averaged SH intensity from the sample was then normalized to that from the quartz reference, thus reducing the effect of laser beam fluctuations. The input polarization was set by a half-wave plate and the output SH polarization was selected with an analyzer with the fundamental and harmonic beams polarized either parallel (*P*) or perpendicular (*S*) to the plane of incidence. To directly compare the SH intensities generated from the MCT and the quartz samples, it is essential that there is no alteration in the optical train between the two different measurements. This ensures that the beam intensity profile of the incident beam has not changed in either case. The quartz sample was oriented such that the fundamental and the harmonic beams were polarized parallel to the X-dielectric axis. In this configuration, the quartz d_{11} coefficient was measured. A Maker fringe pattern was obtained on rotating about the quartz (010) surface around the X-dielectric axis with the intensity value for quartz taken from analysis of the envelope of the Maker fringes. For this particular quartz sample the slab thickness was such that the Maker Fringe envelope maximized at normal incidence (Fig. 2). The MCT sample on the other hand was mounted on a stage that allowed rotation of the sample around the sample

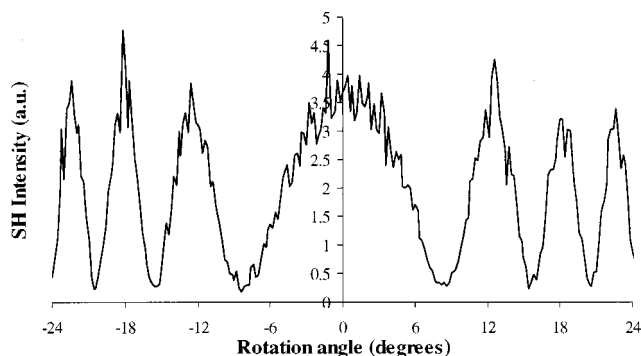


FIG. 2. Maker fringe obtained for the quartz reference sample on rotation around the X dielectric axis.

TABLE I. Measured SH intensities at the rotation angles corresponding to Fig. 3(a).

Rotation angle	$P_{IN} - P_{OUT} I_{MCT}^{2\omega}$ (a.u.)
45°	0.0060 ± 8%
225°	0.0090 ± 8%
315°	0.0167 ± 8%

surface normal. The incidence angle was fixed at 45° (±0.3°). Both the quartz and the MCT samples were located at the focal point of a lens of 50 cm focal length ensuring that the photon flux was identical in both cases. The only difference between the geometries was the position of the analyzer and the PMT for the collection of the transmitted and the reflected SH signals from the quartz and the MCT samples, respectively.

RESULTS AND DISCUSSION

The rotational anisotropy patterns for the MCT epilayer measured in air in the $P_{IN} - P_{OUT}$ (*P*-polarized fundamental in the *P*-polarized second harmonic out) and in the $P_{IN} - S_{OUT}$ polarization configurations are shown in Figs. 3(a) and 3(b), respectively. Details of the generation of such rotational patterns for MCT including descriptions of the sample and its surface preparation can be found elsewhere.⁷⁻⁹ The absence of an even fourfold symmetry pattern indicates the MCT surface to be vicinal and so not a true (100) surface. Based on the work by Yamada and Kimura¹⁰ the anisotropy patterns were modeled to obtain the orientation and tilt angles of the vicinal surface, $\psi = 55^\circ$ and $\delta = 2.3^\circ$, respectively (see Fig. 1). It is also worth pointing out that at zero degrees rotation, the incident fundamental beam is colinear with the crystal *x* axis which is defined as the [100] crystal direction. Tables I and II show the reflected SH intensities for the MCT sample positioned at each of the anisotropy maxima corresponding to the rotation angles in Fig. 3(a) and 3(b). For the quartz, the intensity of the transmitted signal was found to be stable to within 5% over the measurements taken before and after each set of MCT measurements and over two complete sets of measurements on different days. In arbitrary units, which are the same as those used in Fig. 3, the quartz intensity was

$$I_{Quartz}^{2\omega} = 3.46 \pm 5\% .$$

As noted above, to evaluate the effective bulk *d* coefficient for MCT, it is necessary to compare the reflected second harmonic intensity from the sample with the intensity generated by the same beam when transmitted through quartz. The

TABLE II. Measured SH intensities at the rotation angles corresponding to Fig. 3(b).

Rotation angle	$P_{IN} - S_{OUT} I_{MCT}^{2\omega}$ (a.u.)
0°	0.0189 ± 8%
90°	0.0113 ± 8%
180°	0.0083 ± 8%
270°	0.0161 ± 8%

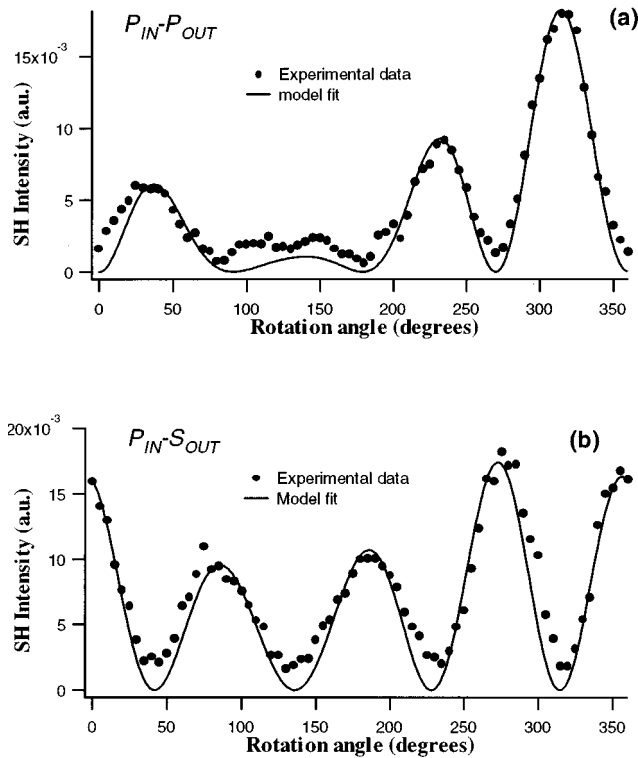


FIG. 3. Comparison of experimental and theoretical fitting of the rotational anisotropy pattern for a vicinal MCT (100) sample. The measurements were performed in air in both the (a) $P_{IN}-P_{OUT}$ and (b) $P_{IN}-S_{OUT}$ polarization configurations at an incidence angle of 45° .

calculation is formally based on the plane wave approximation. In the calculations of Jerphagnon and Kurtz¹¹ the same approximation is made in calculating the Maker fringe intensities in transmission through a slab, but corrections are subsequently applied to allow for the Gaussian profile of the beams and for multiple reflections. With most experimental setups these corrections are small. In the present procedure, the corrections can legitimately be taken as part of the quantity K , given below in Eqs. (1) and (2). Given that the beam profile remains reasonably constant for transmission through a thin slab and that the multiple internal reflections will contribute to both transmitted and reflected second harmonic, the assumption that the quantity K can be canceled between the equations for the reflected and transmitted intensities to produce Eq. (10) below is partially justified. The quantitative values of the corrections that should be applied to the plane wave approximation are not at present known, but should not be larger than those applied in the Kurtz–Jerphagnon method, and are known not to be critical. The results quoted below are for a plane wave fundamental of angular frequency, ω incident at an angle θ on a plane surface. Bound and free second harmonic refracted waves are generated and the requirements of the boundary conditions for the second harmonic at the entry face lead to the generation of a second harmonic reflected wave. The exit face plays no part in the calculation of the reflected signal. For the quartz reference Maker fringe calculation, the transmitted wave is calculated by solving the boundary conditions at the exit face, leading

to the equation of Jerphagnon and Kurtz¹¹ for the Maker fringe envelope. Both calculations have been carried out explicitly starting with the same formula for the fundamental incident wave, to ensure that the “front factors” in the formulas for the intensities (which appear differently in various publications) are at least obtained on the same basis for the two cases. The calculation is a rather simplified example of the Jerphagnon–Kurtz procedure, since the material is isotropic, and the details are not given here.

For the experimental setup described above, the transmitted SH intensity at normal incidence takes the form,^{11,12}

$$I_{\text{Quartz}}^{2\omega} = K8E_0^4 \left(\frac{2}{1+n_\omega} \right)^4 \frac{n_\omega(n_\omega+n_{2\omega})(n_\omega+1)}{(1+n_{2\omega})^3(n_{2\omega}^2-n_\omega^2)^2} (d_{11})^2$$

$$= KV_{\text{Quartz}}(d_{11})^2 E_0^4, \quad (1)$$

where K is a constant factor which takes into account, as discussed above, various properties of the incident beam profile and n_ω and $n_{2\omega}$ are the appropriate refractive indices of the quartz material at the fundamental and harmonic frequencies. E_0 is the incident electric field amplitude and d_{11} is the relevant d coefficient for quartz. The formulas given below for the calculation of the reflected wave refer to the “laboratory coordinate system” where z is the normal to the entry face, x is in the entry face and in the plane of incidence, and y is in the entry face and normal to the plane of incidence. The angle of incidence and reflection at both frequencies is θ and the angles of refraction at the fundamental and second harmonic frequencies are, respectively, θ'_ω and $\theta'_{2\omega}$.

The first step in the calculation is to transform the second order susceptibility tensor from the standard crystal coordinate system to the above laboratory system. In the crystal system the only nonzero values, $\chi_{ijk}^{(2)} = d = d_{36}$, occur when ijk are all different. If we write $\chi_{ijk}^{(2)} = \chi'_{ijk}d$ the transformation matrix for χ'_{ijk} depends only on the Miller indices of the chosen entry face, the angle of rotation about the surface normal, and the vicinal angle. Details of the transformation are given in the Appendix. The vicinal angle is determined by fitting the SHG intensity pattern (see Fig. 3).

The reflected second harmonic intensity may be written in the general form,

$$I_{\text{MCT}}^{2\omega} = KR_B^2 t_A^4 \frac{1}{(n_{2\omega}^2 - n_\omega^2)^2} d^2 E_0^4$$

$$= KV_{\text{MCT}} [d_{36}(\text{MCT})]^2 E_0^4, \quad (2)$$

where A and B stand for either S - or P -type polarization. The transmission factor for the amplitude of the fundamental wave (polarization type A) entering the surface is t_A and R_B is the factor governing the generation of the reflected second harmonic wave (polarization type B).

The formulas for the evaluation of these quantities for both polarizations are summarized below.

$$t_S = \frac{2 \cos \theta}{(n_\omega \cos \theta'_\omega + \cos \theta)},$$

$$t_P = \frac{2 \cos \theta}{(n_\omega \cos \theta + \cos \theta')}, \quad (3)$$

and

$$R_S = \left(\frac{g_x - p_y n_{2\omega} \cos \theta'_{2\omega}}{n_{2\omega} \cos \theta'_{2\omega} + \cos \theta} \right),$$

$$R_P = \left(\frac{f_x n_{2\omega} - g_y \cos \theta'_{2\omega}}{n_{2\omega} \cos \theta + \cos \theta'_{2\omega}} \right), \quad (4)$$

where

$$f_x = \frac{1}{n_{2\omega}^2} \{ (n_{\omega}^2 \sin^2 \theta'_{\omega} - n_{2\omega}^2) p_x + (n_{\omega}^2 \cos \theta'_{\omega} \sin \theta'_{\omega}) p_z \},$$

$$f_z = \frac{1}{n_{2\omega}^2} \{ (n_{\omega}^2 \sin \theta'_{\omega} \cos \theta'_{\omega}) p_x + (n_{\omega}^2 \cos^2 \theta'_{\omega} - n_{2\omega}^2) p_z \}, \quad (5)$$

and

$$g_x = n_{\omega} p_y \cos \theta'_{\omega},$$

$$g_y = n_{\omega} (p_z \sin \theta'_{\omega} - p_x \cos \theta'_{\omega}). \quad (6)$$

The nonlinear polarization is given by

$$p_i = \chi'_{ijk} (e_{\omega})_j (e_{\omega})_k. \quad (7)$$

In Eq. (7), where the repeated index summation convention applies, the components of the unit polarization vectors are

$$(e_{\omega})_x = -\cos \theta'_{\omega}, \quad (e_{\omega})_y = 0, \quad (e_{\omega})_z = \sin \theta'_{\omega} \quad (8)$$

for *P*-type input and

$$(e_{\omega})_x = 0, \quad (e_{\omega})_y = 1, \quad (e_{\omega})_z = 0 \quad (9)$$

for *S*-type input.

The quantities V_{Quartz} and $V_{\text{(MCT)}}$ in Eqs. (1) and (2) can be calculated for each geometry from the measured angles and refractive indices. The MCT *d* coefficient can thus be deduced from,

$$d_{36}(\text{MCT}) = \left(\frac{I_{\text{MCT}}^{2\omega}}{I_{\text{quartz}}^{2\omega}} \right)^{1/2} \left(\frac{V_{\text{Quartz}}}{V_{\text{MCT}}} \right)^{1/2} d_{11}(\text{Quartz}). \quad (10)$$

For quartz, using the optical index values of $n_{\omega} = 1.53413$ and $n_{2\omega} = 1.54702$ at normal incidence, $V_{\text{Quartz}} = 143.85$. In the case of MCT, the rotational position of the sample was taken into account along with the fact that the MCT (100) surface is vicinal. Thus using values of $n_{\omega} = 3.54$ and $n_{2\omega} = 3.485$ (Ref. 13) at a rotation angle of 315° in the $P_{\text{IN}}-P_{\text{OUT}}$ configuration, $V_{\text{MCT}} = 4.415 \times 10^{-7}$. Therefore $d_{36} = 377$ pm/V for a value of 0.3 pm/V employed for the quartz d_{11} coefficient.¹⁴ This exercise was repeated for each of the intensities reported in Tables I and II and the calculated values compared. The average value is thus

$$d_{36} = 350 \pm 40 \text{ pm/V}.$$

The value 350 ± 40 pm/V is the largest so far measured for zinc-blende type compounds with values for d_{36} of 170 pm/V and 109 pm/V for GaAs¹⁴ and CdTe,¹⁴ respectively, at the fundamental wavelength of 1064 nm (1.166 eV). However, it is worth noting that both GaAs and CdTe are transparent at 1.166 eV whereas MCT is already strongly absorbing,¹⁴ with an absorption coefficient of $4.7 \times 10^4 \text{ cm}^{-1}$. At the harmonic frequency (2.33 eV) both GaAs² and CdTe¹⁴ are absorbing with coefficients of 1.2

$\times 10^5 \text{ cm}^{-1}$ and $6 \times 10^4 \text{ cm}^{-1}$, respectively, while MCT has an even higher value of $3.3 \times 10^5 \text{ cm}^{-1}$. These large absorption coefficient values indicate that the magnitude of the measured d_{36} coefficient arises from a delicate interplay between the resonance enhancement of the coefficient and the absorption process. The harmonic wavelength at 532 nm lies in the vicinity of the E_1 electronic transition in MCT, which occurs at the Λ position in the Brillouin zone.¹⁵ It is interesting to note that the highest values calculated at resonance for the *d* coefficient of CdTe, at the Γ position at the center of the Brillouin zone, did not exceed 120 pm/V.¹⁶ Hence the incorporation of mercury atoms at a mole fraction of 0.72 in MCT, so increasing the proportion of HgTe units in the MCT lattice enhances the polarizability. Furthermore, the reduced symmetry away from the center of the Brillouin zone combines to yield a *d*-coefficient value three times as large as that for CdTe.

CONCLUSIONS

The second order nonlinear coefficient (d_{36}) of the narrow-band gap semiconductor, mercury cadmium telluride (MCT), has been measured for the first time. Due to the high absorption coefficient of the MCT at both the fundamental and harmonic wavelengths, the measurement was performed by comparing the second harmonic intensity reflected from the MCT surface to the second harmonic intensity measured for a quartz sample in transmission. The analysis carried out depends on the derivation of comparable expressions for the reflected and transmitted intensities and using this approach a value of $d_{36}(\text{MCT}) = 350 \pm 40$ pm/V is obtained. This is much larger than other *d* coefficients reported for similar zinc-blende type materials and the large magnitude of the MCT d_{36} coefficient is attributed to an electronic resonance enhancement.

APPENDIX: ORIENTATION OF CRYSTAL SURFACE AND TRANSFORMATION OF THE $\chi^{(2)}$ TENSOR

In the standard crystal coordinate system, the \mathbf{d} matrix for SHG for the zinc-blende structure has the form:

$$\mathbf{d} = \begin{pmatrix} 0 & 0 & 0 & 1 & 0 & 0 \\ 0 & 0 & 0 & 0 & 1 & 0 \\ 0 & 0 & 0 & 0 & 0 & 1 \end{pmatrix} \mathbf{d} = \mathbf{d}' \mathbf{d}.$$

The dimensionless matrix \mathbf{d}' is written in three dimensional form as χ' . The surface normal \mathbf{n} is specified by the Miller indices of the surface and a reference axis \mathbf{r} in the surface (orthogonal to \mathbf{n}) is chosen by inspection. For example, if the surface were the (111) plane then the reference axis could be taken as $[\bar{1}01]$. A third orthogonal axis is set up as $\mathbf{n} \times \mathbf{r}$. The vectors are normalized and their components define the transformation matrix \mathbf{T} . The transformed χ' tensor in the laboratory coordinate system is then obtained as,

$$\mathbf{R}_z(\varphi) \mathbf{R}_y(\delta) \mathbf{R}_z(\psi) \mathbf{T} \chi',$$

where the \mathbf{R} are rotation matrices about the successively transformed axes. The $\mathbf{R}_z(\psi)$ rotation orients the surface so that the vicinal tilt is in the *x* direction (rotation about *y*),

given by $\mathbf{R}_y(\delta)$, and the variation corresponding to the abscissas in Fig. 1 is effected by the rotation $\mathbf{R}_z(\varphi)$.

A program has been written that performs these operations for any surface in cubic, tetragonal, or orthorhombic crystals. In the particular case considered here, the Miller indices define the (100) surface, the reference axis is [100], and the best fit to the anisotropy pattern is obtained for $\psi = 55^\circ$ and $\delta = 2.3^\circ$.

ACKNOWLEDGMENT

The authors are grateful to the Defense and Evaluation Research Agency, Malvern, UK for providing the IMPMOVPE sample used in this study.

¹P. D. Maker, R. W. M. Nisenhoff, and C. M. Savage, *Phys. Rev. Lett.* **8**, 121 (1962).

²Y. Hase, K. Kumata, S. S. Kano, M. Ohasi, T. Kondo, R. Ito, and Y. Shiraki, *Appl. Phys. Lett.* **61**, 145 (1992).

³B. Fluegel, A. Mascarenhas, J. F. Geisz, and J. M. Olsen, *Phys. Rev. B* **57**, R6787 (1998).

⁴N. Bloemberger and P. S. Pershan, *Phys. Rev.* **128**, 606 (1962).

⁵J. Tunnicliffe, S. J. C. Irvine, O. D. Dosser, and J. B. Mullin, *J. Cryst. Growth* **68**, 245 (1984).

⁶R. W. Boyd, *Nonlinear Optics* (Academic, London, 1992).

⁷F. Jackson, P. V. E. Elfick, L. E. A. Berlouis, P. F. Brevet, A. A. Tamburello-Luca, P. Hébert, and H. H. Girault, *J. Chem. Soc., Faraday Trans.* **92**, 4061 (1996).

⁸L. E. A. Berlouis, A. W. Wark, F. R. Cruickshank, D. Pugh, and P. F. Brevet, *J. Electron. Mater.* **28**, 830 (1999).

⁹A. W. Wark, Ph.D. thesis, University of Strathclyde, Glasgow, UK, 2000.

¹⁰C. Yamada and T. Kimura, *Phys. Rev. B* **49**, 14372 (1994).

¹¹J. Jerphagon and S. K. Kurtz, *J. Appl. Phys.* **41**, 1667 (1970).

¹²P. Pavlides and D. Pugh, *J. Phys.: Condens. Matter* **3**, 967 (1991).

¹³P. M. Amiritharaj, *Handbook of Optical Constants II*, edited by E. D. Palik (Academic, New York, 1991), pp. 655–689.

¹⁴I. Shoji, T. Kondo, A. Kitamoto, M. Shirane, and R. Ito, *J. Opt. Soc. Am. B* **14**, 2268 (1997).

¹⁵R. R. Galazka and A. Kisiel, *Phys. Status Solidi* **34**, 63 (1969).

¹⁶E. Ghahramani, D. J. Moss, and J. E. Sipe, *Phys. Rev. B* **43**, 9700 (1991).